



## Original Article

# Anti-inflammatory Effects of Tabersonine in Rheumatoid Arthritis



Ruo-Jia Zhang<sup>1</sup>, Shu-Feng Li<sup>2</sup>, Hao-Jun Shi<sup>3</sup>, Jian-Li Zhao<sup>2</sup>, Yun Geng<sup>4</sup>, Huan-Cai Fan<sup>1</sup>, Yu-Ang Zhang<sup>1</sup>, Dan-Dan Shi<sup>1</sup>, Ting Wang<sup>1</sup>, Xi-Feng Li<sup>1</sup>, Ting-Ting Zhang<sup>1</sup>, Ji-Hong Pan<sup>1,5</sup>, Lu-Na Ge<sup>1,5</sup> and Jin-Xiang Han<sup>1,5\*</sup>

<sup>1</sup>Biomedical Sciences College & Shandong Medicinal Biotechnology Centre, Key Lab for Biotech-Drugs of National Health Commission, Key Lab for Rare & Uncommon Diseases of Shandong Province, Shandong First Medical University & Shandong Academy of Medical Sciences, Jinan, China; <sup>2</sup>Department of Orthopedic Surgery, The First Affiliated Hospital of Shandong First Medical University, Jinan, China; <sup>3</sup>The second clinical medical college, Henan University of Chinese Medicine, Zhengzhou, China; <sup>4</sup>Shandong First Medical University & Shandong Academy of Medical Sciences, Jinan, China; <sup>5</sup>Department of Rheumatology and Autoimmunology, The First Affiliated Hospital of Shandong First Medical University, Jinan, China

Received: February 04, 2022 | Revised: March 22, 2022 | Accepted: April 02, 2022 | Published: April 29, 2022

## Abstract

**Background and objectives:** Tabersonine (Tab), an indole alkaloid, is a traditional Chinese medicine that can be used as an anti-inflammatory agent and is mainly isolated from the medicinal plant *Catharanthus roseus*.

**Methods:** To develop safer and more promising new treatments for arthritis, we tested the biological activity of Tab against rheumatoid arthritis fibroblast-like synoviocytes (RA-FLS) and evaluated its effect on the progression of rheumatoid arthritis through animal experiments. The mechanism of Tab in rheumatoid arthritis (RA) was further clarified by network prediction and a series of molecular biology experiments.

**Results:** The results showed that Tab inhibited the proliferation, migration, invasion and other biological functions of RA-FLS, effectively reducing the expression of inflammatory factors in RA-FLS and the number of vascular loops in 1730 cells in vitro. In vivo, Tab significantly reduced paw and joint swelling and inhibited inflammatory cytokine expression in collagen-induced arthritis model mice. Preliminary mechanistic studies showed that Tab inhibited the expression and activation of key molecules in the PI3K pathway, suggesting that Tab influences the progression of RA disease by inhibiting the PI3K-Akt signaling pathway.

**Keywords:** Tabersonine; RA; RA-FLSs; PI3K-AKT.

**Abbreviations:** AKT, phosphorylation and protein kinase B; bDMARDs, biological agents DMARDs; CIA, collagen-induced arthritis; CREB, CAMP Responsive Element Binding Protein; csDMARDs, conventional synthetic DMARDs; Dac, Dactolisib; DMARDs, disease-modifying anti-rheumatic drugs; ELISA, Enzyme-linked immunosorbent assay; IL1 $\beta$ , human interleukin 1 beta; IL6, interleukin 6; IL8, interleukin 8; LPS, lipopolysaccharide; MIP-2, C-X-C Motif Chemokine Ligand 2; MMP3, matrix metalloproteinase 3; PDGF, platelet-derived growth factor; PDK1, pyruvate dehydrogenase kinase 1; PI3K, phosphatidylinositol-4,5-bisphosphate 3-kinase; PIP3, phosphatidylinositol 3,4,5-trisphosphate; qRT-PCR, quantitative real-time polymerase chain reaction; RA, rheumatoid arthritis; RA-FLS, rheumatoid arthritis fibroblast-like synoviocytes; Tab, Tabersonine; TGF- $\beta$ , transforming growth factor-beta; TNF- $\alpha$ , tumor necrosis factor-alpha; tsDMARDs, targeted synthetic DMARDs.

\*Correspondence to: Jin-Xiang Han, Biomedical Sciences College & Shandong Medicinal Biotechnology Centre, Key Lab for Biotech-Drugs of National Health Commission, Key Lab for Rare & Uncommon Diseases of Shandong Province, Shandong First Medical University & Shandong Academy of Medical Sciences, Jinan 250017, China; Department of Rheumatology and Autoimmunology, The First Affiliated Hospital of Shandong First Medical University, Jinan 250017, China. ORCID: <https://orcid.org/0000-0003-0227-9757>. Tel: +86-531-59567360, Fax: +86-531-59567355, E-mail: sams\_h2016@163.com

**How to cite this article:** Zhang RJ, Li SF, Shi HJ, Zhao JL, Geng Y, Fan HC, et al. Anti-inflammatory Effects of Tabersonine in Rheumatoid Arthritis. *J Explor Res Pharmacol* 2022;7(3):125–132. doi: 10.14218/JERP.2022.00013.

**Conclusions:** In general, Tabersonine can be used as a new potential treatment for RA.

## Introduction

Rheumatoid arthritis (RA) is a chronic inflammatory disease that is characterized by synovial hyperplasia, high levels of T cells, B cells, and monocytes, and the subsequent destruction of articular cartilage.<sup>1</sup> The pannus tissue formed by the lining of a synovial membrane is enriched with fibroblast-like synoviocytes (FLSs), which can secrete large amounts of proinflammatory cytokines to cause local and systemic inflammation.<sup>2</sup>

Disease-modifying anti-rheumatic drugs (DMARDs), one of the main treatment drugs for rheumatoid arthritis at present, can be divided into conventional synthetic DMARDs (csDMARDs),

biological agents DMARDs (bDMARDs), and targeted synthetic DMARDs (tsDMARDs). However, clinical studies have shown that almost 30% of patients have adverse reactions or poor responses to csDMARDs and bDMARDs. Therefore, identifying a novel method to inactivate the pathological activity of FLSs in RA may provide novel treatment strategies.<sup>3</sup>

Previous studies have identified lots of inflammatory signaling pathways, including PI3K-AKT in RA, and inhibition of these pathways has been confirmed to effectively improve the symptoms of RA.<sup>4</sup> Bartok *et al*. reported that PI3K $\delta$  was highly expressed in RA-FLS. Except for phosphatidylinositol-4,5-bisphosphate 3-kinase gamma (PI3K $\gamma$ ), PI3K alpha (PI3K $\alpha$ ) and PI3K beta (PI3K $\beta$ ) were also expressed in RA-FLS.<sup>5</sup> Human interleukin 1beta (IL1 $\beta$ ) and tumor necrosis factor-alpha (TNF- $\alpha$ ) selectively induced PI3K $\delta$  expression, while platelet-derived growth factor (PDGF) and transforming growth factor-beta (TGF- $\beta$ ) did not.<sup>6</sup> Dactolisib (Dac) is a dual ATP-competitive PI3K inhibitor that inhibits PI10  $\alpha/\gamma/\delta/\beta$ . PI3K is an intracellular phosphatidylinositol kinase with serine/threonine kinase activity.<sup>7</sup> Activated PI3K converts PIP2 to phosphatidylinositol 3,4,5-trisphosphate (PIP3), the latter of which acts as an anchor to promote pyruvate dehydrogenase kinase 1 (PDK1) phosphorylation and protein kinase B (AKT) activation.<sup>8</sup> AKT is the main downstream effector of PI3K, and the activation of AKT further induces the NF- $\kappa$ B or mTOR signaling pathways, which are closely related to inflammation.<sup>9</sup> In addition to the pro-inflammatory role of PI3K-AKT in RA, it also serves as the target to validate the therapeutic effects of promising treatment drugs in RA.

The Tab is an indole alkaloid mainly isolated from the medicinal plant *Catharanthus roseus*.<sup>10</sup> Previous studies have shown that Tab can inactivate the NF- $\kappa$ B signaling pathway and inhibit the production of proinflammatory mediators. However, its exact role in RA remains unclear. In this study, we evaluated whether Tab can protect against RA progression by inhibiting the pathogenic behavior of RA-FLS.

## Materials and methods

### Network pharmacology

The ingredients were input into the PubChem database to search chemical structure formula, Smiles files, molecular weight, PubChem CID, etc., to prepare parameters and files required for target prediction. Using the InDraw web version (<http://indrawforweb.integre.com/>) draw Tab chemical structure. Through TCMSP (<http://lsp.nwu.edu.cn/tcmsp.php>), STITCH (<http://stitch.embl.de/>), Swiss Target Prediction (<http://www.swisstargetprediction.ch/>), PubChem (<https://pubchem.ncbi.nlm.nih.gov/>), DTPS (<http://demo.dtps.iprexmed.com/>) forecast composition of targets database. The repeated values were deleted after the action targets of each component were combined. Rheumatoid arthritis-related targets are searched by keyword "Rheumatoid", and all are summarized and sorted according to gene names through GeneCards (<https://www.genecards.org/>), the NCBI-Gene (<https://www.ncbi.nlm.nih.gov/gene>), DrugBank (<https://www.drugbank.ca/>), OMIM (<https://www.omim.org/>). The predicted targets were compared with those related to rheumatoid arthritis, and the repeated targets were identified by the Venn diagram. These overlapping targets were the targets of Tab on the potential treatment of RA. Using OmicShare (<http://www.omicshare.com/>) online tools for these targets for dynamic GO and KEGG enrichment analysis. PPI networks of target genes were obtained by interactive gene/protein

retrieval tools from STRING (<https://cn.string-db.org/>).<sup>11</sup>

### Cell culture and arthritis models

The synovial tissues were collected during knee joint replacement surgery (n = 16; 6 males, 10 females, age 33–75, average age 55). All patients met the diagnostic criteria for RA as revised at the American College of Rheumatology in 1987. Written informed consent was obtained from each patient, and all samples were processed anonymously. Synovial tissue was treated with collagenase II and III (Solarbio, China, 6 h later after harvest), for RA-FLS extraction.<sup>12</sup>

### Stimulation assays

As previously described, primary RA-FLS was isolated and cultured, and cells between passages 3 and 7 were used in experiments.<sup>11</sup> Our experiments showed that many inflammatory factors can effectively stimulate RA-FLS to simulate the inflammatory microenvironment, including IL1 $\beta$ , TNF- $\alpha$ , and lipopolysaccharide (LPS), which exhibit the greatest effects. RA-FLS were grown at a suitable density on 24-well plates and stimulated with inflammatory factors for 24 h. Activation of PI3K/AKT pathways was blocked using dactolisib (Dac, BEZ235, Selleck).<sup>13</sup>

### Cytotoxicity test and cell viability

RA-FLS was seeded into 96-well plates with a density of  $3 \times 10^3$  cells per well and was exposed to DMSO or Tab in different concentrations of 0–50  $\mu$ M. Each well was incubated with 10  $\mu$ l of Cell count Kit -8 (CCK-8) reagent for more than 1 hour, and the OD value in each well was measured at 450 nm with a microplate reader to detect cell proliferation rate for 24–72 h. The concentration of Tab was determined by cell growth rate. For cell viability measurement by CCK-8, RA-FLS with similar density above were challenged by IL1 $\beta$  (10  $\mu$ g/ml) and TNF- $\alpha$  (10  $\mu$ g/ml) before Tab (20  $\mu$ M) treatment.

In addition, RA-FLS, treated as described above, in 96-well plates were subjected to a 5-ethyl-2-deoxyuridine (EDU) assay (C10310-1, RiboBio), and the proliferation efficiency of RA-FLS was detected by a high-intensity screening (HCS) system.<sup>14</sup>

### Migration, invasion, and angiogenesis experiment

RA-FLS was divided into the normal control group, inflammatory stimulation group (IL1 $\beta$ , 10  $\mu$ g/ml), and Tab (20  $\mu$ M) treatment group with IL1 $\beta$  stimulation. Trypsin cells were inoculated in chambers, and cell density was adjusted to  $3 \times 10^4$  cells/well. After adherence to the chamber wall, 200  $\mu$ l serum-free medium was replaced. 10–12 hours later, the cells were fixed with 4% paraformaldehyde for 30 minutes, stained with crystal violet for 40 minutes, and observed under a microscope to observe the number of cell migration. The matrix glue was diluted with medium 1:8 and evenly spread in chambers for invasion analysis.

Then, HUVEC-1730 cells were plated in 6-well plates with a density of  $4 \times 10^4$  cells per well and were treated and grouped as described above for 24 h.<sup>15</sup> The matrix gel was prepared at a 1:1 volume ratio with medium, and 180–200  $\mu$ l was added to each well in a 48-well plate, and the plate was placed in an incubator for 4 hours until the matrix gel completely solidified. Then, the treated

**Table 1.** The primers used are listed in qRT-PCR

Gene Name	Sense (5'-3')	Antisense (5'-3')
GAPDH	GCACCGTCAAGGCTGAGAAC	TGGTGAAGACGCCAGTGG
IL6	ACTCACCTCTTCAGAACGAA TTG	CCATCTTTGGAAGGTTCAAGTTG
IL8	CCAGGAAGAAACCACCG	GGTGGAAAGGTTTGGAGTAT
MMP3	CTGGACTCCGACACTCTGGA	CAGGAAAGGTTCTGAAGTGACC
PIP3	TCCGCTGCTTTATCAGGTCG	CACGAACTCGATGGGGATGA
MIP-2	CAGCCAGA TGCA TCAA TGCC	TGGAA TCCTGAACCCACTTCT
PDK1	AGGACAAAAGTGCTGAGGATG	CCATGTTCTTCTAGGCCCTTCATA
CREB	CCAAGTTGTTGTTCAAGGTACTCA	TTCAAATTCAGTACATCTGCT

cells were placed on the matrix gel at a density of  $1 \times 10^4$  cells per well. After 2 hours, tube formation in the HUVEC-1730 cells was observed by microscopy.

#### **Quantitative real-time polymerase chain reaction (qRT-PCR)**

RNA was extracted with TRIZOL and RNA concentration and purity were detected. The purity of RNA was best when A260/A280 was between 1.8 and 2.0. cDNA was synthesized with 1 µg RNA by HiScript<sup>®</sup> III RT SuperMix for qPCR (Vazyme, R323-01), which the procedure was 50°C, 15min; 85°C, 5 sec. And PCR (Basel Roche 480, Switzerland) was performed using an SYBR Green Mastermix kit (Cwbio, China) as a template.<sup>16</sup> The primers used are listed in Table 1.

#### **Western blot analysis**

The total cell lysates were separated by sodium dodecyl. After protein quantification by the BCA protein quantification method, samples were loaded and separated by SDS-PAGE gel (12% separated gel and 10% concentrated gel) at 66 V for 10 min, 76 V for 20 min, 126 V for 1 h. Then, the protein samples were electrophoretically transferred onto 0.45 µm polyvinylidene fluoride (PVDF) membranes (Millipore, Bedford, MA, USA). Then, the PVDF membranes were blocked and incubated at 4°C overnight with primary antibodies and secondary antibodies for 1 h. The blots were visualized using an enhanced chemiluminescent substrate (ECL) kit (Vazyme, Nanjing, China). The protein bands were quantified using ImageJ software 2.0 (National Institutes of Health, Bethesda, Maryland, USA) and were normalized to the density of the respective GAPDH band.

The following antibodies were used: anti-PI3K (1:500, 27921-1-AP, Proteintech), anti-PIP3 (1:1,000, 17552-1-AP, Proteintech), anti-PDK1 (1:500, 10026-1-AP, Proteintech), phospho- PDK1 (1:200, 29241-1-AP, Proteintech), anti-AKT (1:500, MA5-14916, Invitrogen, Thermo Fisher), and phospho-AKT (1:200, 44-621G, Invitrogen, Thermo Fisher). and glyceraldehyde-3-phosphate dehydrogenase (GAPDH) (1:1,000, Proteintech, Wuhan, China).

#### **Collagen-induced arthritis (CIA) model**

CIA is a well-established mouse model of human RA.<sup>17</sup> Arthritic mice develop swollen joints, chronic inflammation, and joint destruction. CIA was induced by injecting type II collagen at 2 mg/mL (Chondrex, Washington, USA) and complete Freud's adjuvant

(Sigma-Aldrich, Mannheim, Germany) in a 1:1 emulsion (200 µl) was injected at the base of the tail of 10-week-old male DBA mice. A type II collagen and incomplete Freud's adjuvant (Sigma-Aldrich) 1:1 emulsion was injected (200 µl) at the base of the tail in 14-week-old mice. The mice were monitored once per day to detect the signs of arthritis.

#### **Hematoxylin-Eosin (H&E) staining**

The elbow and knee joints of mice were fixed with a tissue fixator for 24 h and decalcified in 10% EDTA solution for 30 days. During this period, the decalcification solution was replaced. The sample was dehydrated and paraffin-embedded. After dewaxing, the slices were stained with hematoxylin at 37°C for 5 min, washed with tap water for 10 min, immersed in alcohol containing 1% hydrochloric acid for 5 s, then rinsed with tap water for 10 min, and washed with distilled water for 1–2 s. Stain 120 s with 5% eosin. Dehydrate with 70%, 80%, 90%, and 95% diluted alcohol for 5 minutes, followed by 100% alcohol for 10 minutes. The slices were cleaned with xylene for 10 minutes to dewax and then coated with neutral balm. After drying, the tissues of each group were observed under a light microscope.<sup>3</sup>

#### **Enzyme-linked immunosorbent assay (ELISA)**

The supernatant of the above cells cultured for 24 hours was collected and evaluated by ELISA kits (Dakewe). Supernatants were obtained from the eyeballs of mice 50 days after the second collagen injection, and the inflammatory factor content in the supernatant was detected by ELISA.

#### **Immunofluorescence microscopy**

RA-FLS was plated in 48 wells at a density of  $1 \times 10^4$  cells per well. After treatment of 24 hours, the cells were immobilized, perforated with Triton X-100, and incubated with a secondary antibody (1:500, Invitrogen, Thermo Fisher) at 37°C for 1 hour. Finally, DAPI staining was performed. The nuclear translocation of AKT was observed under a fluorescence microscope.

#### **Statistical analysis**

Data were expressed as the mean ± standard deviation (SD). All data were analyzed by SPSS 25.0. Statistical differences between

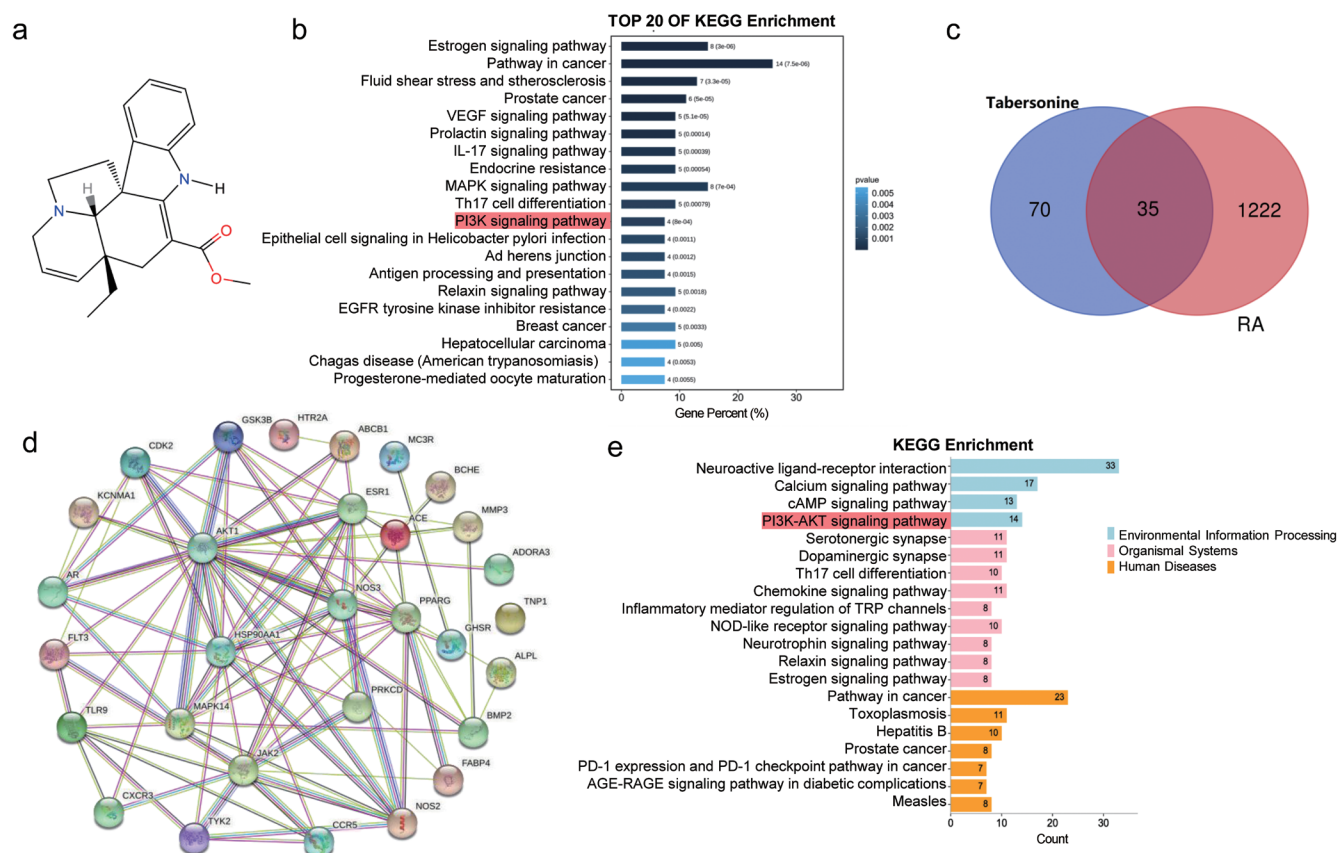


**Fig. 1. Network prediction of Tab and RA-related pathways.** (a) The 2D chemical formula for Tab. (b) KEGG analysis of sequencing data. (c) The overlapping genes of RA and Tab are represented by the Venn diagram. (d) PPI analysis through STRING on key molecules that Tab might affect. (e) KEGG enrichment analysis was performed for overlapping genes, and the first 20 were selected according to P-value for visual analysis. RA, rheumatoid arthritis; Tab, Tabersonine.

the two groups were firstly selected by t-test and multiple groups were assessed by ANOVA.  $P$ -value  $\leq 0.05$  was considered to be significant.

## Results

### Network prediction of Tab and RA-related pathways

We obtained the molecular formula of Tab from PubChem and use InDraw online version (<http://indrawforweb.integle.com/>) to map the Tab 2D chemical structure (Fig. 1a). Through Tab sequencing data, we performed KEGG analysis on differentially expressed genes in RA-FLS and found that the IL17 signaling pathway, MAPK signaling Pathway, and PI3K signaling Pathway were enriched (Fig. 1b). 70 potential targets of Tab were predicted by TCMSP, STITCH, Swiss Target Prediction, PubChem, and DTSP databases. Furthermore, 1,222 genes related to RA were predicted by NCBI-Gene, DrugBank, and OMIM database. The Venn diagram (Fig. 1c) shows that a total of 35 genes have been predicted as the potential therapeutic targets of Tab in RA. We also applied STRING to construct a PPI network that showed that these potential targets, such as Hsp90, GSK3 $\beta$ , etc., were related to PI3K or involved in the PI3K-AKT signaling pathway (Fig. 1d). KEGG (Fig. 1e) analysis of overlapping genes was performed by Omic-

Share, and these genes were associated with a variety of human diseases and metabolism, such as metabolic diseases, and degenerative diseases. In addition, consistent with the KEGG analysis of sequencing data, the network predicted KEGG enrichment and also identified THE PI3K signaling pathway as a potential therapeutic target for Tab.

### Tabersonine influenced the biological activity of RA-FLS

In order to determine the therapeutic effect of Tab on RA-FLS, a cytotoxicity test was firstly carried out, and 20  $\mu$ M was finally selected for subsequent experiments (Fig. 2a). CCK-8 (Fig. 2b) and EDU (Fig. 2c) were used to determine cell viability and proliferation. The results showed that the cell viability and proliferation with the activation of IL1 $\beta$  were significantly decreased when RA-FLS were treated by Tab compared with its parental control. In addition, the expression of interleukin 6 (IL6), interleukin 8 (IL8), and matrix metalloproteinase 3 (MMP3) in RA-FLS were all decreased upon Tab treatment (Fig. 2d). The tube formation assay of HUVEC-1730 showed that Tab could also inhibit the pro-angiogenesis properties of RA-FLS (Fig. 2e). The results of cell migration and invasion experiments (Fig. 2f) showed that the number of cell migration and invasion increased significantly after the addition of inflammatory factors. However, such increases were attenuated by the Tab treatment.



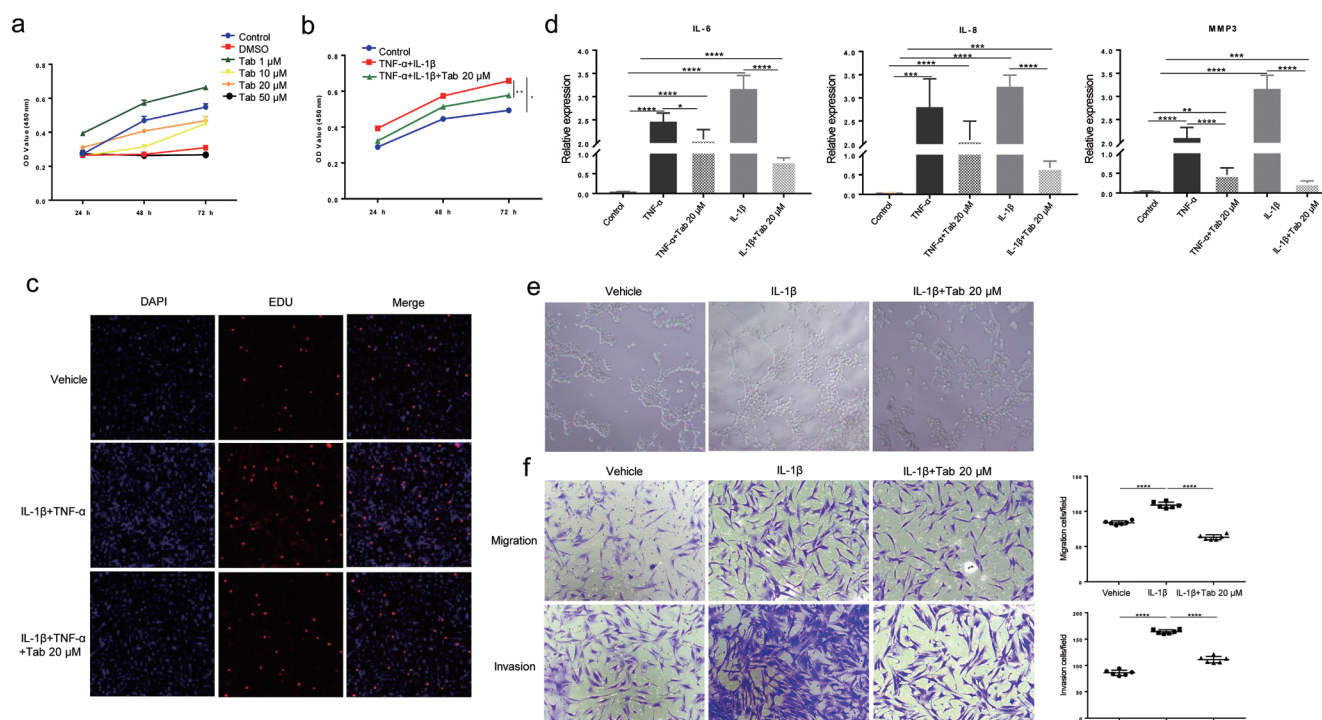


**Fig. 2. The effect of Tab on the bioactivity of RA-FLS.** (a) RA-FLS was stimulated with IL1 $\beta$  (10  $\mu$ g/ml) and TNF- $\alpha$  (10  $\mu$ g/ml) for 24 h and then incubated with Tab (20  $\mu$ M) for 24 h. Then, CCK-8 was used to analyze the cytotoxicity of Tab on RA-FLS. (b) The proliferation rate of RA-FLS was detected by CCK-8 at 24 h, 48 h, and 72 h. (c) EDU working solution (50 nM) was used to label cells for 8 h and to detect the proliferation of RA-FLS. (Blue: DAPI; Red: EDU) (d) With the activation of IL1 $\beta$  (10  $\mu$ g/ml) and TNF- $\alpha$  (10  $\mu$ g/ml) respectively, RA-FLS were treated by Tab (20  $\mu$ M). Then, the expression levels of IL6, IL8, and MMP-3 RNA were measured in RA-FLS. (e) The 1730 cells were treated by the supernatant from RA-FLS as treated above to determine their tube-forming ability. (f) The migration and invasion abilities of RA-FLS cells were observed under a 10 $\times$  microscope and counted with an average of four fields per well. The data are the mean  $\pm$  SEM, \* $p$  < 0.005, \*\* $p$  < 0.01, \*\*\* $p$  < 0.001, \*\*\*\* $p$  < 0.00001,  $n$  = 3. IL1 $\beta$ , human interleukin 1 $\beta$ ; IL6, interleukin 6; IL8, interleukin 8; MMP3, matrix metalloproteinase 3; RA-FLS, rheumatoid arthritis fibroblast-like synoviocytes; Tab, Tabersonine; TNF- $\alpha$ , tumor necrosis factor- $\alpha$ .

### Tabersonine ameliorates the CIA inflammatory phenotype

To further determine the therapeutic effect of Tab on RA, CIA model mice were established, and Tab was added for the intervention. The results showed that Tab inhibited the arthritic parameters of the RA-like phenotype, as evidenced by the decreased degree of ankle swelling, paw thickness, and arthritis score (Fig. 3b), compared to the control group with DMSO treatment.

HE staining showed that synovial hyperplasia, inflammatory cell infiltration, and cartilage destruction were all ameliorated in Tab-inoculated mice (Fig. 3c). Serum of the CIA models with or without Tab treatment was collected for ELISA analysis. The data showed that the expression of inflammatory factors, such as IL1 $\beta$  and TNF- $\alpha$  was decreased in Tab treated group compared to the CIA model group (Fig. 3d). In addition, the three-dimensional spiral structure of the tibia edge was analyzed by the micro-CT method. Compared to the control group, the relative bone volume (BV/TV), and trabecular separation (Tb.Sp) in the CIA model group increased significantly and trabecular bone mineral density (Tb.BMD) reduced. But the addition of the Tab could rescue these changes.

### Tab protects against RA progression through PI3K signaling

To detect the effects of Tab on the PI3K pathway, we detected the

expression levels of inflammatory factors downstream of PI3K. The results showed that the mRNA expression levels of PIP3, PDK1, C-X-C Motif Chemokine Ligand 2 (MIP-2), and CAMP Responsive Element Binding Protein (CREB) were significantly increased after the addition of IL1 $\beta$ , whereas the above increases were all suppressed following the exposure of Tab (Fig. 4a).

Secondly, protein levels were detected. The expression levels of PIP3, PDK1, and p-PDK1 increased after the addition of IL1 $\beta$ . However, such increases were suppressed when RA-FLS were challenged by Tab simultaneously, while the change of AKT was not significant. We also detected changes in phosphorylation levels of this molecule and found that the phosphorylation levels of AKT were consistent with the above trend (Fig. 4b). This indicates that Tab can indeed regulate the expression level of PI3K related molecules in RA-FLS.

To detect whether Tab inactivated RA-FLS via the PI3K pathway, Dac, an inhibitor of PI3K, was introduced to block the PI3K pathway in the absence or presence of Tab. The data showed that Dac could inactivate the PI3K pathway as efficiently as Tab. However, no additive suppression was observed. With the stimulation of IL1 $\beta$ , the expression level of IL6, IL8, and MMP3 decreased significantly in Tab-treated RA-FLS when compared to its parental control. However, no further decreases were found when RA-FLS were treated by both of them (Fig. 4c). Similar effects on the expression of parameters downstream of the PI3K pathway, including PIP3, PDK1, MIP-2, and CREB were also observed (Fig. 4d).

Western results showed that the expression level of p-AKT was

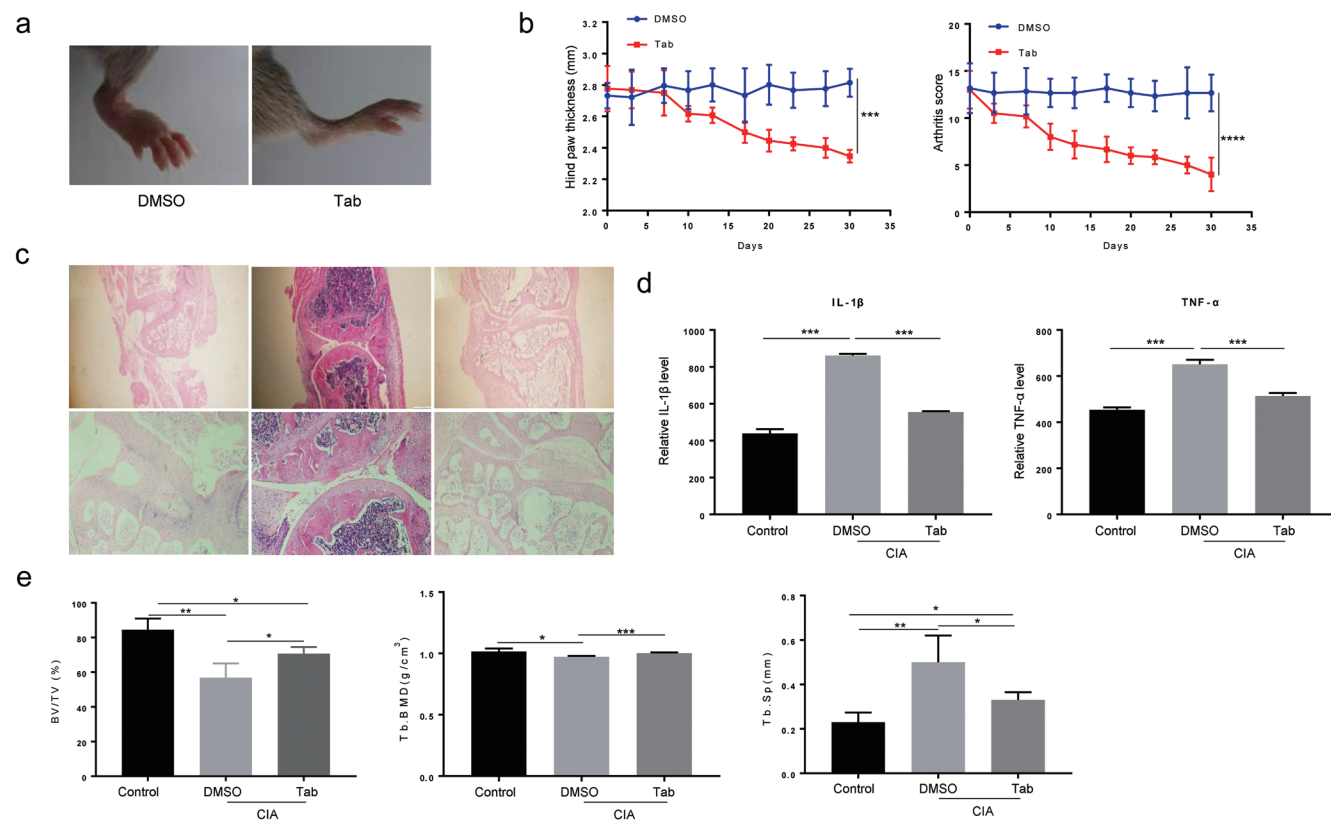


**Fig. 3. The effects of Tab on the disease progression in CIA mice.** Arthritis was induced by collagen in DBA mice. (a) Representative rear paw photographs Tab treatment group and its parental controls. (b) The degree of fore and hind paw thickness was measured. Arthritis was evaluated as 0 (no swelling) to 4 (strong swelling) once per day by two independent observers under blinded conditions. The severity of edema and paw redness was assessed once per day. All results are presented as the mean  $\pm$  SEM of three independent experiments performed in triplicate. (c) Hematoxylin slides were blindly tested by trained observers to determine the proliferation and invasion of RA-FLS, and also the destruction of articular and bone destruction. (d) Blood samples were collected from eyeballs, and the expression levels of inflammatory factors in serum were detected by ELISA kits. (e-g) Representative Micro-CT images of hindlimbs and interphalangeal joints. Micro-CT and 3D reconstruction techniques were used to determine the bone volume fraction (BV/TV), trabecular bone density (Tb.BMD), and trabecular separation (Tb.Sp). The data are the mean  $\pm$  SEM, \* $p < 0.005$ , \*\* $p < 0.01$ , \*\*\* $p < 0.001$ , \*\*\*\* $p < 0.00001$ ,  $n = 3$ . CIA, collagen-induced arthritis; Dac, Dactolisib; ELISA, Enzyme-linked immunosorbent assay; IL1 $\beta$ , human interleukin 1 $\beta$ ; RA-FLS, rheumatoid arthritis fibroblast-like synoviocytes; Tab, Tabersonine; TNF- $\alpha$ , tumor necrosis factor- $\alpha$ .

increased under the stimulation of IL1 $\beta$ , but decreased with the addition of an inhibitor or Tab. However, no further changes were observed when RA-FLS were treated by both of them. In addition, the total protein level of AKT did not change significantly after treatment (Fig. 4e).

Furthermore, immunofluorescence was used to detect the nuclear translocation of AKT (Fig. 4f). The data showed that the nuclear staining of AKT increased obviously when RA-FLS were exposed to IL1 $\beta$ , but the addition of Dac or Tab can inhibit the nuclear translocation of AKT. However, no further decrease of nuclear translocation of AKT was observed when Tab-exposed RA-FLS were challenged by Dac further.

### Future directions

In this study, Tab has been identified that could ameliorate the inflammatory phenotype of RA-FLS by inactivating the PI3K-AKT signaling pathway and thus delaying the disease process of RA. However, some drawbacks need to be resolved in future studies. To confirm the therapeutic effects of Tab on RA were achieved by

PI3K, the exactly targeted proteins should be predicted and validated. Furthermore, RNA-sequencing should also be included to predict the potential activity and signaling pathways of Tab in RA.

### Conclusions

Rheumatoid arthritis is an autoimmune disease characterized by synovial hyperplasia and an inflammatory phenotype. It often manifests as symmetric polyarthritis, accompanied by synovial joint swelling and pain,<sup>18</sup> especially in hand and foot joints, but other tissues and organs, such as blood vessels and peripheral nerves, can also be involved. Currently, the treatment of RA mainly includes drug therapy, including nonsteroidal anti-inflammatory drugs, DMARDs, glucocorticoids, and biological agents.<sup>19,20</sup> However, traditionally used drugs induce side effects that are harmful to the kidney, stomach, and liver.<sup>12,21</sup> In recent years, the treatment of RA by Chinese herbal medicine has been increasingly favored by the majority of patients with rheumatism because traditional Chinese herbal medicine has curative effects, safety, and nontoxic side effects.<sup>22</sup> Our study found that Tab inhibits the inflammatory

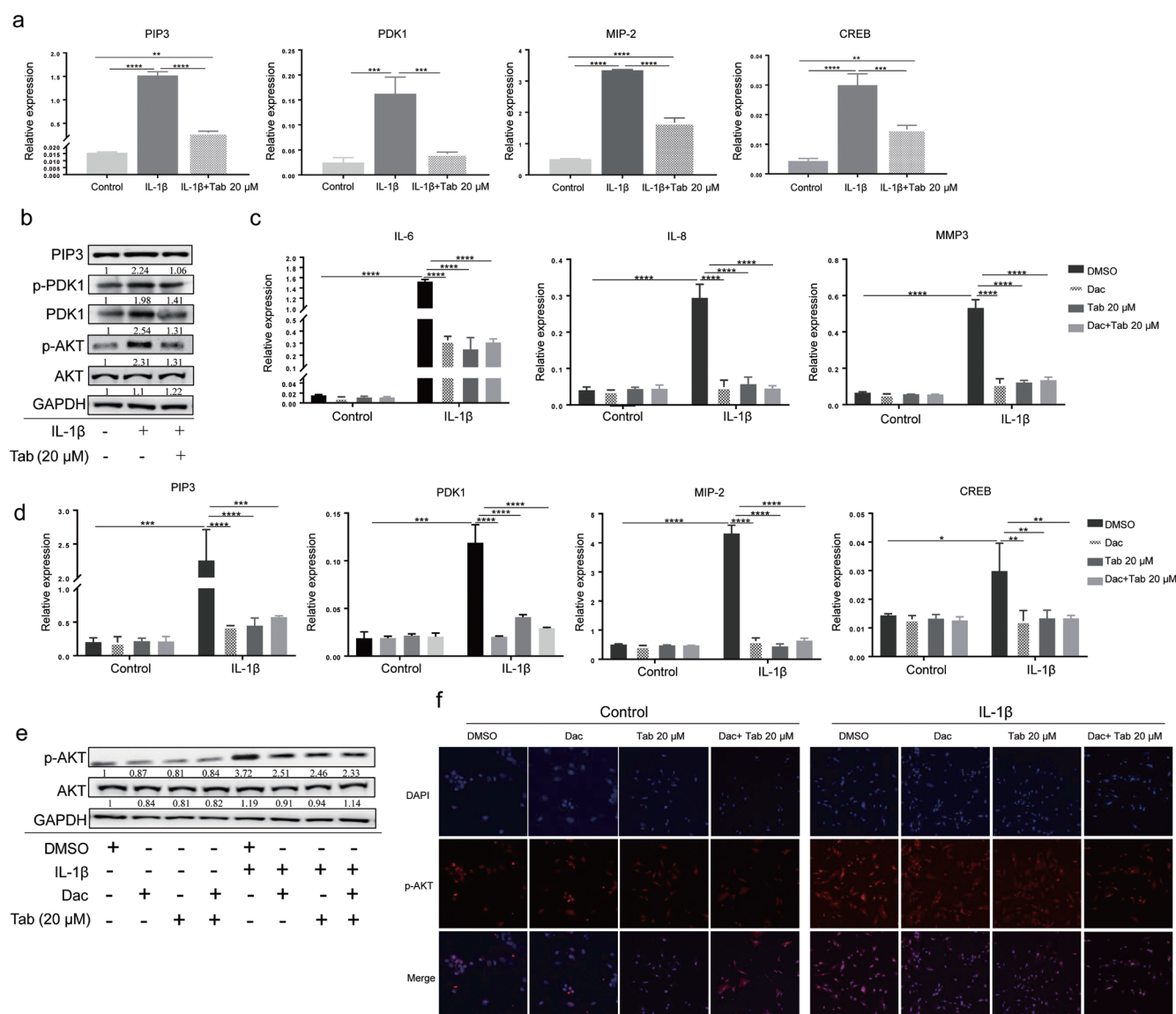


**Fig. 4. Tab protects against RA progression via PI3K signaling.** (a) The RNA expression levels of PIP3, PDK1, MIP-2, and CREB were measured in RA-FLS 24 h after treatment with IL1 $\beta$  (10  $\mu$ g/ml), then incubated and subsequent Tab (20  $\mu$ M). (b) RA-FLS was treated with IL1 $\beta$  (10  $\mu$ g/ml), and subsequent Tab (20  $\mu$ M) for 36–48 h, the protein expression levels of PIP3, PDK1, p-PDK1, AKT, and p-AKT were detected by Western Blot, and the bands were digitally quantified. The Control group was set to “1”. With or without IL1 $\beta$  (10  $\mu$ g/ml) stimulation, RA-FLS was incubated with PI3K inhibitor- Dac (5nM) or Tab (20  $\mu$ M) or treated with a combination of both. (c) The RNA expression levels of IL6, IL8, and MMP-3. (d) The RNA expression levels of PIP3, PDK1, MIP-2, and CREB. (e) The protein expression of AKT and p-AKT. The bands were digitally quantified and the Control group was set to “1”. (f) Fluorescence microscopy was used to detect nuclear translocation of activated AKT. (Blue: DAPI; Red: AKT) The data are the mean  $\pm$ SEM, \* $p$  < 0.005, \*\* $p$  < 0.01, \*\*\* $p$  < 0.001, \*\*\*\* $p$  < 0.00001, n = 3. CREB, CAMP Responsive Element Binding Protein; Dac, Dactolisib; IL1 $\beta$ , human interleukin 1 $\beta$ ; IL6, interleukin 6; IL8, interleukin 8; MIP-2, C-X-C Motif Chemokine Ligand 2; MMP3, matrix metalloproteinase 3; PI3K, phosphatidylinositol 4,5-bisphosphate 3-kinase; PIP3, phosphatidylinositol 3,4,5-trisphosphate; qRT-PCR, quantitative real-time polymerase chain reaction; RA, rheumatoid arthritis; RA-FLS, rheumatoid arthritis fibroblast-like synoviocytes; Tab, Tabersonine; TNF- $\alpha$ , tumor necrosis factor- $\alpha$

response and arthritis progression by inhibiting the pathogenic activity of RA-FLS, suggesting that Tab is a potential drug for the treatment of RA.

The Tab is a terpenoid indole alkaloid found in a variety of plants, including *C. roseus* (Apocynaceae). Previous studies have shown that Tab has strong anti-inflammatory properties and protects the lung from injury by inactivating the NF- $\kappa$ B and P38/MK2 pathways.<sup>23</sup> Our data showed that Tab exerts its anti-inflammatory

effect by inhibiting the activity of the PI3K-AKT signaling pathway and that the PI3K-Akt signaling pathway is required for Tab conferred protection against acquiring the inflammatory phenotype of RA-FLS, further confirming its likelihood as a treatment drug for RA.

In summary, Tab has proven to be a promising candidate for developing novel therapies for RA because it can ameliorate the inflammatory phenotype of RA-FLS.



## Acknowledgments

None.

## Funding

This research was funded by the Taishan Scholar Project of Shandong Province (No. tsqn20161076), Natural Science Foundation of Shandong Province (Grant No. ZR2020YQ55), the Innovation Project of Shandong Academy of Medical Sciences, the Youth Innovation Technology Plan of Shandong University (2019KJK003) and Academic Promotion Programmer of Shandong First Medical University (LJ001).

## Conflict of interest

The authors have no conflict of interest related to this publication.

## Author contributions

Contributed to study concept and design (RJZ, LNG, and JXH), acquisition of the data (HJS, HCF, DDS, TW, XFL, and TTZ), assay performance, and data analysis (RJZ, YAZ, JHP, and LNG), drafting of the manuscript (RJZ and JXH), critical revision of the manuscript (RJZ, LNG, and LNG) supervision (JHP and JXH), material support (SRL, JLZ, and YG). All authors have made a significant contribution to this study and approved the final manuscript.

## Data sharing statement

The data used to support the findings of this study are included in the article.

## References

- [1] Klareskog L, Lundberg K, Malmström V. Autoimmunity in rheumatoid arthritis: citrulline immunity and beyond. *Adv Immunol* 2013;118:129–158. doi:10.1016/B978-0-12-407708-9.00003-0, PMID:23683943.
- [2] Zhang D, Li X, Hu Y, Jiang H, Wu Y, Ding Y, *et al*. Tabersonine attenuates lipopolysaccharide-induced acute lung injury via suppressing TRAF6 ubiquitination. *Biochem Pharmacol* 2018;154:183–192. doi:10.1016/j.bcp.2018.05.004, PMID:29746822.
- [3] Ho Lee Y, Gyu Song G. Comparative efficacy and safety of tofacitinib, baricitinib, upadacitinib, filgotinib and peficitinib as monotherapy for active rheumatoid arthritis. *J Clin Pharm Ther* 2020;45(4):674–681. doi:10.1111/jcpt.13142, PMID:32495356.
- [4] Feng FB, Qiu HY. Effects of Artesunate on chondrocyte proliferation, apoptosis and autophagy through the PI3K/AKT/mTOR signaling pathway in rat models with rheumatoid arthritis. *Biomed Pharmacother* 2018;102:1209–1220. doi:10.1016/j.biopha.2018.03.142, PMID:29710540.
- [5] Folkes AJ, Ahmadi K, Alderton WK, Alix S, Baker SJ, Box G, *et al*. The identification of 2-(1H-indazol-4-yl)-6-(4-methanesulfonyl-piperazin-1-ylmethyl)-4-morpholin-4-yl-thieno[3,2-d]pyrimidine (GDC-0941) as a potent, selective, orally bioavailable inhibitor of class I PI3 kinase for the treatment of cancer. *J Med Chem* 2008;51(18):5522–5532. doi:10.1021/jm800295d, PMID:18754654.
- [6] Maimud CJ. The PI3K/Akt/PTEN/mTOR pathway: a fruitful target for inducing cell death in rheumatoid arthritis? *Future Med Chem* 2015;7(9):1137–1147. doi:10.4155/fmc.15.55, PMID:26132523.
- [7] Xie Y, Shi X, Sheng K, Han G, Li W, Zhao Q, *et al*. PI3K/Akt signaling transduction pathway, erythropoiesis and glycolysis in hypoxia (Review). *Mol Med Rep* 2019;19(2):783–791. doi:10.3892/mmr.2018.9713, PMID:30535469.
- [8] Falke JJ, Ziemba BP. Interplay between phosphoinositide lipids and calcium signals at the leading edge of chemotaxing amoeboid cells. *Chem Phys Lipids* 2014;182:73–79. doi:10.1016/j.chemphyslip.2014.01.002, PMID:24451847.
- [9] Chen K, Lin ZW, He SM, Wang CQ, Yang JC, Lu Y, *et al*. Metformin inhibits the proliferation of rheumatoid arthritis fibroblast-like synoviocytes through IGF-IR/PI3K/AKT/m-TOR pathway. *Biomed Pharmacother* 2019;115:108875. doi:10.1016/j.biopha.2019.108875, PMID:31028998.
- [10] Kai T, Zhang L, Wang X, Jing A, Zhao B, Yu X, *et al*. Tabersonine inhibits amyloid fibril formation and cytotoxicity of Aβ(1–42). *ACS Chem Neurosci* 2015;6(6):879–888. doi:10.1021/acschemneuro.5b00015, PMID:25874995.
- [11] Aihaiti Y, Song Cai Y, Tuerhong X, Ni Yang Y, Ma Y, Shi Zheng H, *et al*. Therapeutic Effects of Naringin in Rheumatoid Arthritis: Network Pharmacology and Experimental Validation. *Front Pharmacol* 2021;12:672054. doi:10.3389/fphar.2021.672054, PMID:34054546.
- [12] Wang L, Song G, Zheng Y, Wang D, Dong H, Pan J, *et al*. miR-573 is a negative regulator in the pathogenesis of rheumatoid arthritis. *Cell Mol Immunol* 2016;13(6):839–849. doi:10.1038/cmi.2015.63, PMID:26166764.
- [13] Shi F, Zhang J, Liu H, Wu L, Jiang H, Wu Q, *et al*. The dual PI3K/mTOR inhibitor dactolisib elicits anti-tumor activity *in vitro* and *in vivo*. *Oncotarget* 2018;9(1):706–717. doi:10.18632/oncotarget.23091, PMID:29416647.
- [14] Zeng C, Pan F, Jones LA, Lim MM, Griffin EA, Sheline YI, *et al*. Evaluation of 5-ethynyl-2'-deoxyuridine staining as a sensitive and reliable method for studying cell proliferation in the adult nervous system. *Brain Res* 2010;1319:21–32. doi:10.1016/j.brainres.2009.12.092, PMID:20064490.
- [15] Lennikov A, Mirabelli P, Mukwaya A, Schappner M, Thangavelu M, Lachota M, *et al*. Selective IKK2 inhibitor IMD0354 disrupts NF-κB signaling to suppress corneal inflammation and angiogenesis. *Angiogenesis* 2018;21(2):267–285. doi:10.1007/s10456-018-9594-9, PMID:29332242.
- [16] Chen X, Xie R, Gu P, Huang M, Han J, Dong W, *et al*. Long Noncoding RNA *LBCS* Inhibits Self-Renewal and Chemoresistance of Bladder Cancer Stem Cells through Epigenetic Silencing of SOX2. *Clin Cancer Res* 2019;25(4):1389–1403. doi:10.1158/1078-0432.CCR-18-1656, PMID:30397178.
- [17] Miyoshi M, Liu S. Collagen-Induced Arthritis Models. *Methods Mol Biol* 2018;1868:3–7. doi:10.1007/978-1-4939-8802-0\_1, PMID:30244448.
- [18] Aletaha D, Neogi T, Silman AJ, Funovits J, Felson DT, Bingham CO 3rd, *et al*. 2010 Rheumatoid arthritis classification criteria: an American College of Rheumatology/European League Against Rheumatism collaborative initiative. *Arthritis Rheum* 2010;62(9):2569–2581. doi:10.1002/art.27584, PMID:20872595.
- [19] Scott DL, Wolfe F, Huizinga TW. Rheumatoid arthritis. *Lancet* 2010;376(9746):1094–1108. doi:10.1016/S0140-6736(10)60826-4, PMID:20870100.
- [20] Kumar LD, Karthik R, Gayathri N, Sivasudha T. Advancement in contemporary diagnostic and therapeutic approaches for rheumatoid arthritis. *Biomed Pharmacother* 2016;79:52–61. doi:10.1016/j.biopha.2016.02.001, PMID:27044812.
- [21] Emery P, Pope JE, Kruger K, Lippe R, DeMasi R, Lula S, *et al*. Efficacy of Monotherapy with Biologics and JAK Inhibitors for the Treatment of Rheumatoid Arthritis: A Systematic Review. *Adv Ther* 2018;35(10):1535–1563. doi:10.1007/s12325-018-0757-2, PMID:30128641.
- [22] Lü S, Wang Q, Li G, Sun S, Guo Y, Kuang H. The treatment of rheumatoid arthritis using Chinese medicinal plants: From pharmacology to potential molecular mechanisms. *J Ethnopharmacol* 2015;176:177–206. doi:10.1016/j.jep.2015.10.010, PMID:26471289.
- [23] Zhang D, Li X, Hu Y, Jiang H, Wu Y, Ding Y, *et al*. Tabersonine attenuates lipopolysaccharide-induced acute lung injury via suppressing TRAF6 ubiquitination. *Biochem Pharmacol* 2018;154:183–192. doi:10.1016/j.bcp.2018.05.004, PMID:29746822.